Application of Infrared Thermography technique for the monitoring of Cold Metal Transfer (CMT) joining of aluminium to galvanized steel

Renil Thomas KIDANGAN [1], Sreedhar UNNIKRISHNAKURUP [2], Nithin P. V [1], Krishnan BALASUBRAMANIAM [1], Prabhu RAJAGOPAL [1], K.V. PHANI PRABHAKAR [3], G. PADMANABHAM [3]

[1] Indian Institute of Technology Madras, Chennai, India

[2] Federal Institute for Metal Research and Testing (BAM), Berlin, Germany

[3] International Advanced Research Centre for Powder Metallurgy and New Materials, Hyderabad, India

Contact e-mail: ktrenil@gmail.com

Abstract. In this study, the feasibility of using non-contact Infrared thermography as a potential tool to monitor the CMT welding process is explored. The presence of internal defects such as porosity, lack of filler material deposition and formation of improper weld bead produce perturbations in the surface temperature which can be identified using an Infrared thermography technique. We present recent results obtained from online monitoring of the dissimilar joining using CMT weld brazing of aluminium and steel using a transmission mode measurement approach. The effect of loss of zinc coating on the weldability of the cold metal transfer joining of aluminium to galvanised steel was investigated. A correlation between measured online thermal indications with the weld anomalies is successfully attempted and the results are compared with the conventional post-weld NDT inspection methods.

Introduction

Replacement of steel by aluminium alloys[1], [2] is of great interest to automotive industry due to light-weighting of automotive bodies thereby improving the efficiency. Due to the difference in physical, mechanical and metallurgical properties between aluminium and steel, the process of joining of these two materials is challenging, mainly minimising formation of brittle intermetallic phases at the Al-Steel interface [3]. Joints with enhanced mechanical performance could be made by employing low heat input process that diminish the intermetallic compound formation and free from spatter. CMT joining process is evolved from the continuous adaptation of the MIG process where the filler wire is intentionally retracted instantaneously after the occurrence of the short circuit [4]–[6]. Cold Metal Transfer (CMT) process invented by Fronius International GmbH is considered as a suitable solution to make a joint between thin sheets of aluminium and steel. So there is a great interest in quantitatively defining the weld joint quality and thus optimizing the weld characteristics. Conventional post weld NDT methods are well established, but consumes time, cost and labour and often weld repairs add to the overheads. In the last few decades several efforts have been reported on the online monitoring of different welding processes

and its ability for detecting defects generated during the welding process. Welding is naturally a high temperature process which emanates high thermal radiations in the weld region. This restricts the employment of conventional contact NDT methods such as ultrasonics, eddy current etc., for real time monitoring. Even a non-contact method such as IR Thermography is adversely influenced by the high thermal radiations from the weld region.

Among the different NDT techniques, the radiation based infrared thermography has the advantage of non-contact measurement quickly. But the major limiting factor in determining the exact surface temperature is emissivity, which depends on metal's chemical structure, its surface roughness, the angle of view, the temperature within the wavelength range of sensor's sensitivity and the presence of oxide films or otherwise coated material on the surface [7]. Over the last few decades infrared sensing technique to welding process monitoring was investigated by many researchers [8]–[17]. Most of this investigations were focused on monitoring from the welding side where the arc is present, but in the present study a different strategy of monitoring is used by looking from the back side and acquired the back surface temperature distribution. In view of the objective of the present study the absolute measurement of temperature is not considered as important as this mode of measuring temperature entails a source of severe errors in as much as with all nonblack bodies, the temperature observed is always below the true temperature owing to deficient emissive power.

In the present work the effect of loss of zinc coating on the weldability of the cold metal transfer joining of aluminium to galvanised steel was investigated using the passive infrared sensing technique. The samples were fabricated and the weld appearance, infrared thermography measurements and radiographic inspection techniques were examined and correlated each other.

2. Experimental Procedure

Experiments were carried out using 1.2 mm thick sheets of aluminium alloy A3003 and 2 mm thick zinc coated steel sheets. Aluminium sheet was placed over the steel sheet with 12.5 mm overlap with nearly zero clearance using a fixture. The welding direction is parallel to the lap seam and the arc is running along the edge of the aluminium sheet. Aluminium alloy A4047 with 12% Si of 1.2mm diameter is used as filler wire. A pure argon shielding environment at a flow rate of 18 L/min were used to deposit the weld. The angle of the torch is 10^{o} to the normal to the welding plate. A Fronius arc welding system (Model 3200) was used to fabricate the joint.

Two Infrared cameras were used for monitoring the welding process. Figure 1 shows the photograph of the experimental setup and figure 2 presents the schematic diagram of the camera positions. First camera was used in reflection mode of inspection where welding torch and the produced weld bead were visible in the thermogram. As the temperature confronted by this camera is high due to the presence of welding arc and the melting of aluminium, the temperature range used was 150^{o}C to 1200^{o}C. The camera was equipped with a filter to reduce the excess irradiations from the welding arc. The acquisition was made at 150 Hz. The second camera was used in transmission mode of inspection where the heat transmitted from the weld zone towards the bottom surface of the steel plate was imaged. The temperature range used in this camera was 20^{o}C to 300^{o}C as the heat transmitted is less compared to the heat at the welding zone. The acquisition frequency for the second case was 127 Hz. In this paper, only the transmission mode of inspection results are discussed.

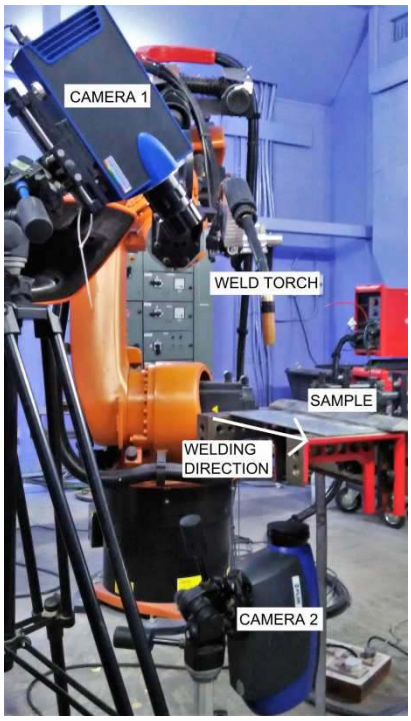

Fig. 1. Experiment setup

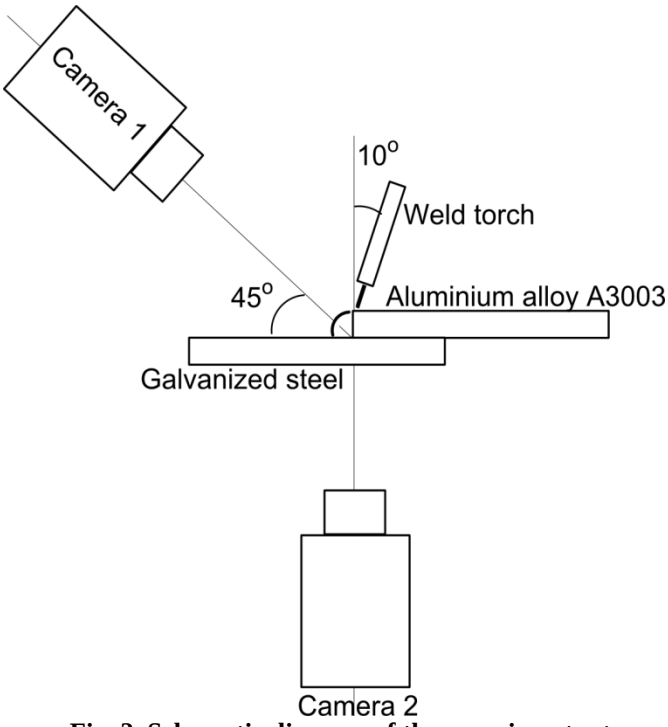

Fig. 2. Schematic diagram of the experiment setup

The objective of this work is to identify the dependency of weld formation towards the presence of zinc coating on the steel plate and how effectively thermography can identify this effect in transmission modes of inspection. In this experimental study, the zinc coating on the steel plate was removed from specific locations by varying the spacing and width of the no-zinc regions. Here two cases were considered.

1. Variation in the width of no-zinc regions keeping the distance between them constant.
2. Variation in the spacing between no-zinc regions keeping the width constant.

Figure 3 shows the schematic top view of the prepared steel samples. All the considered cases were performed at 0.75 m/min welding speed and 4 m/min wire feed rate. Post weld radiographic examinations were also conducted to compare the thermographic data.

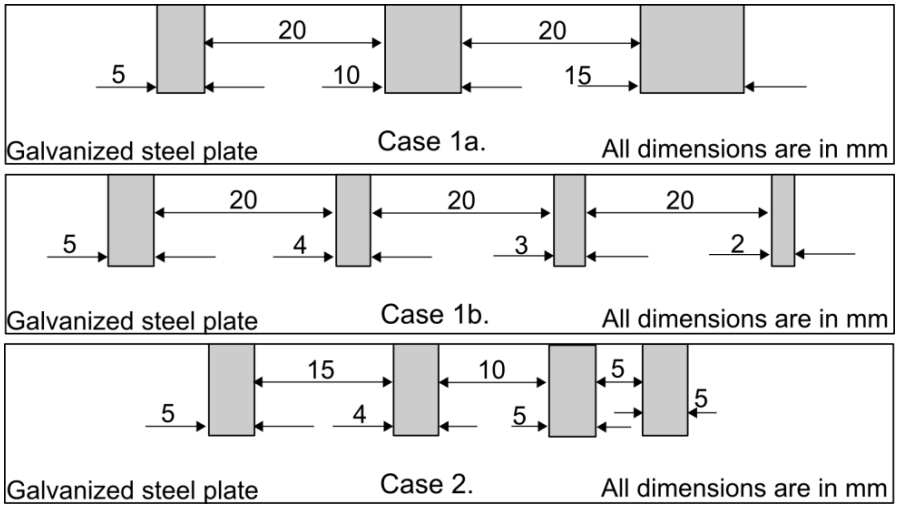

Fig 3. Schematic top view of the prepared samples for different cases

2. Results and discussion

2.1. Weld characteristics based on the observation on the different samples.

a. Smooth flat welds are generated using the CMT welding process. There were no distortion of the weld due to the very small heat input . The zinc coating on the back side of the steel plate was also intact. The bead formed at the steel side showed a wavy nature compared to the more straight one in the aluminium side.
b. From the post processing using radiographic testing, the presence of porosities are observed in the weld bead region. This is attributed to the aluminium oxides. Aluminium oxides contain the hydrogen, which has different solubility in the solid and liquid aluminium. The solid aluminium has a less solubility than that of liquid aluminium. During the solidification process, the excessive atomic hydrogen is expelled from the newly formed solid into the surrounding liquid phase. When the hydrogen reaches a critical solubility level in the liquid, the porosity could be produced in the weld. Furthermore, the entrapment of the shielding gas and/or zinc vapour in the molten pool is another factor for the formation of the porosity [18]
c. The portion of zinc coating is remained during the CMT arc ignition, (after partial vaporization) which improves the wetting capability of the molten filler wire. Without the zinc, the molten filler wire has a very poor wetting capability on the steel. This suggested that a poor wetting over the steel surface occurred and the molten filler wire was poorly bonded with the steel [18]

2.2. Image processing

Figure 4 shows the row thermal image in rainbow colour palette obtained through transmission mode of inspection on an uncoated surface. The pink region with higher temperature in the raw thermal image corresponds to the presence of electrical arc and molten aluminium on the other side of the plate which has travelled a distance of 50 mm from the starting point. It leaves no clue regarding the nature of the weld bead formed during the process which makes image processing an inevitable process.

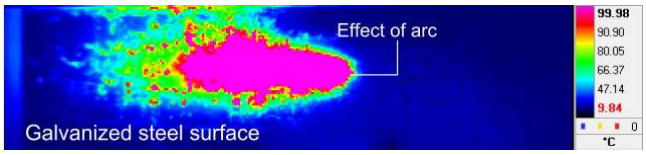

Fig. 4. Row thermal image from the back side of the steel plate showing the effect of arc at a distance of 50mm away from the starting of weld

The primary objective of this work is to identify the no-zinc region which is attributed by the bad formation of weld. The heat flux transferred to the steel surface during welding from both the electrical arc and the molten filler material is transmitted to the rear side and captured using the IR camera. So the rear surface temperature behaviour is expected to contain the anomalies in the weld bead formation and also the fluctuations of the electrical arc. Accordingly the temperature history of a pixel at the rear side of the weld bead on the steel plate contains the effect of poor weld formation. This idea was employed in the image processing algorithm developed using Matlab®. Figure 5 shows the temperature history of ten different points considered along the weld bead on the rear side of the steel plate. The maximum temperature attained by each pixel is at different instances of time which is related to the speed of the welding process. These maximum temperatures of every pixels are aligned in a single frame and the subsequent temperatures in the cooling cycle are shown in consecutive frames. Thus another set of images was created which represents the

cooling of each pixel. The cooling rates are different for each pixel depending upon its locations. The difference between the maximum temperature and the temperature attained after cooling of 1s is plotted and compared with the real and radiographic images of the weld bead.

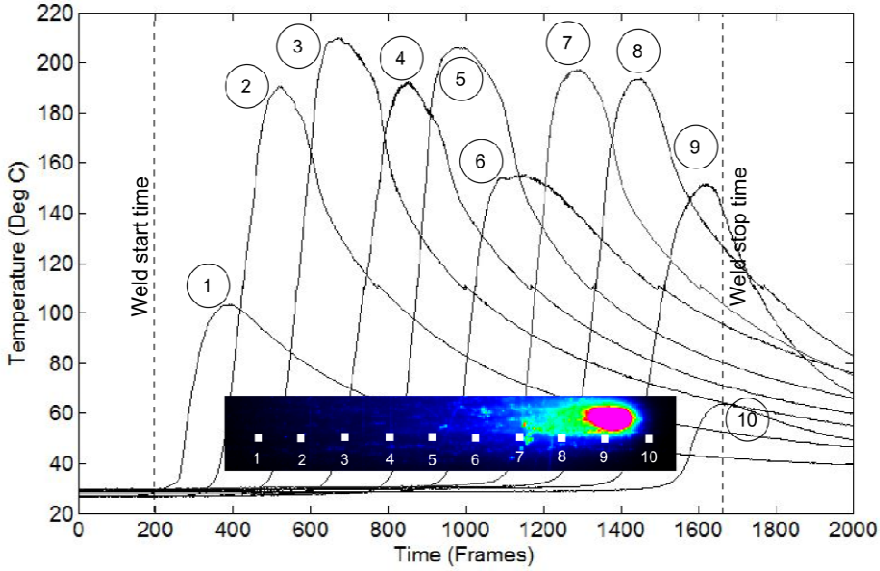

Fig. 5. Temperature history of ten points considered along the bead on the rear side of the steel plate

2.3. Case 1: Variation in the width of no-zinc

Effect on weldability due to the variation in the width of no-zinc regions has been studied on two samples. First sample contains the variations from 15 mm to 5 mm (Case 1a) and the second sample contains the variation from 5 mm to 2 mm (Case 1b). Figure 6 shows the real and radiographic images of Case 1a. The schematic diagram of the sample prepared for Case 1a is shown in figure 3. It consists of three no-zinc regions with widths 5 mm, 10 mm and 15 mm. These regions are named as D1, D2 and D3 respectively. The variation in the bead width can be identified at these locations. The formation of weld bead was seriously affected at these locations.

During the CMT process, the heat energy from the electrical arc cause vaporization of a portion of the zinc coating on the top surface of the steel and a portion of the zinc coating was remained before the short circuit occurred. Then, the molten filler aluminium spread over the top surface of the steel metal under the driving force of surface tension. The wetting of zinc helps to accomplish a brazed aluminium to steel connection. The highly erratic nature of the zinc vapour makes it to counteracts on the arc and the molten metal when it cannot quickly escape from the weld area. This results an unstable arc and the molten droplet has different wetting behaviours, which is responsible for the wavy edge of the weld bead in the steel sample. At the locations where zinc was removed, wetting phenomenon could not happen and this is responsible for the lack of molten metal deposition in these areas as shown in the figure 6.

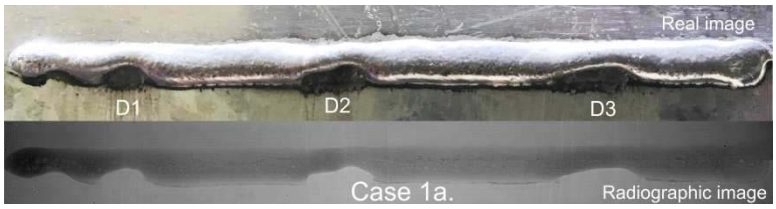

Fig. 6. Real and radiographic images of Case 1a.

As the aluminium molten material was not deposited on the steel surface at the locations given as D1, D2 and D3 in figure, the heat imparted at these locations and thus the transfer of heat to the rear side of the plate will be different from the other regions. This variation was extracted from the acquired back surface temperature using the algorithm explained in the previous section and the obtained image is shown in figure 7.

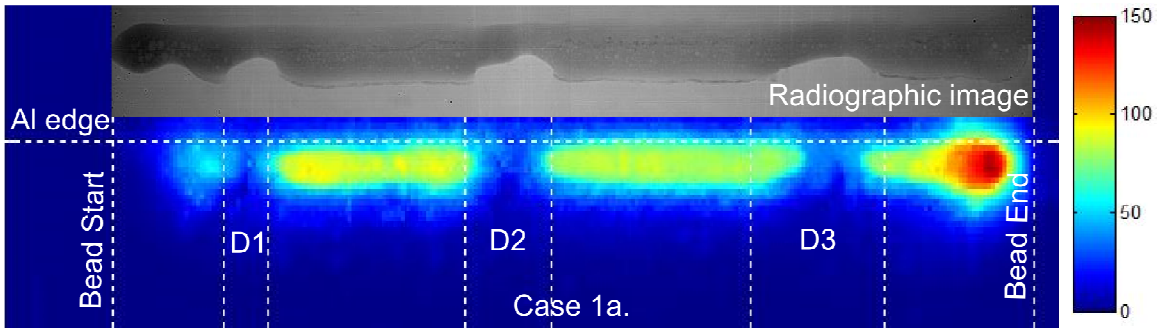

Figure 7. Reconstructed image of Case 1a compared with radiographic image

The thermal contrast between the no-zinc regions and the rest of the bead is evident from the image shown in figure 6. As the molten metal was not deposited on the steel plate at the no-zinc regions, the heat transmitted from these locations to the rear side is less compared to the other part of the bead. This gives clear indications of the variations in the metal deposition.

The welding took place from left to right. The starting and ending of the bead is marked in the processed image. At the bead starting point the effect of material deposit which can be seen in the radiographic image is not visible in the processed image. This corresponds to the common arc stability problem at the beginning of the arc welding process and also which leads to the transfer of less heat into the steel sample and the improper wetting at this portion. At the bead ending side as the weld torch remains stationary for some time, heat imparted at this point is more compared to the rest of the part. The white horizontal dotted line represents the edge of the aluminium plate along which the torch is progressed. As we are imaging the steel surface in transmission mode, the metal deposit information on the aluminium sheet is not accessible to the camera. This explains the visualization of the weld bead below the aluminium edge in the processed image.

Figure 8 shows the real and radiographic images of Case 1b. The schematic diagram of the sample prepared for Case 1b is shown in figure 3. It consists of four no-zinc regions with widths 5 mm, 4 mm, 3 mm and 2 mm. These regions are named as D1, D2, D3 and D4 respectively. As in Case 1a the variation in the bead width can be identified at these locations. Even a 2 mm removal of zinc region is affecting the welding process which demonstrates the effect of zinc on the weldability.

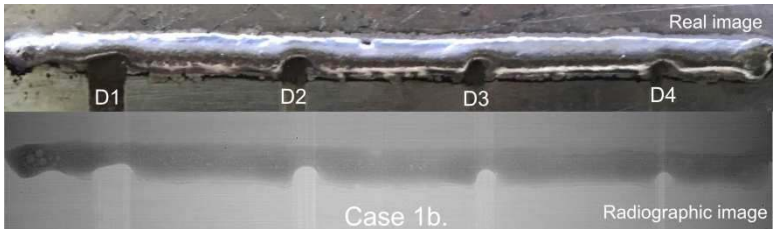

Fig. 8. Real and radiographic images of Case 1a.

Figure 9 shows the reconstructed image of Case 1b. The 2mm perturbation (D4) on the weld bead is clearly visible in the processed image. The observations made in Case 1a is also applicable in Case 1b.

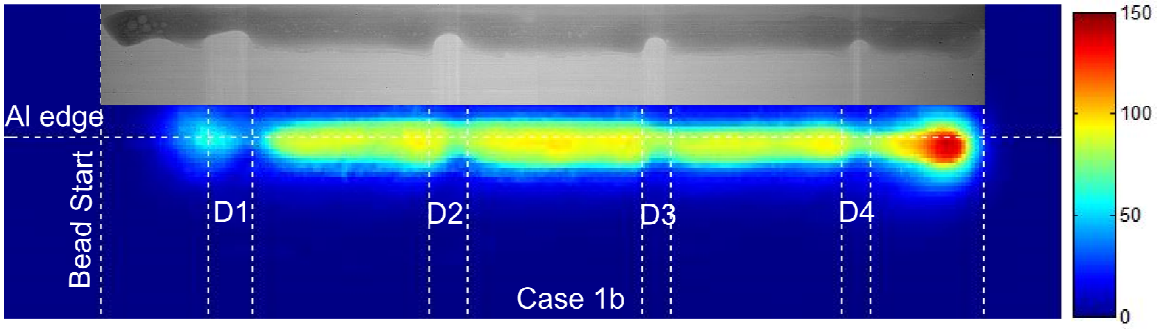

Fig. 9. Reconstructed image of Case 1b compared with radiographic image

2.4. Case 2: Variation in the spacing between no-zinc regions

Figure 10 shows the real and radiographic images of Case 2 where the spacing between the no-zinc regions varied by keeping no-zinc width constant. The schematic diagram of the sample is shown in figure 3. The ability of thermography to differentiate close-lying no-weld regions in transmission mode is explored in this section. A distance of 5 mm between two consecutive no-zinc regions was sensed by the welding process and reflected in the bead formation. This subsequently reflected in the heat transferred to the rear side and imaged using IR camera. The reconstructed image shown in figure 11 reveals the above fact.

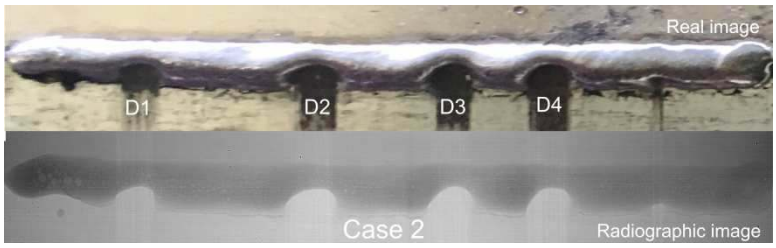

Fig. 10. Real and radiographic images of Case 2

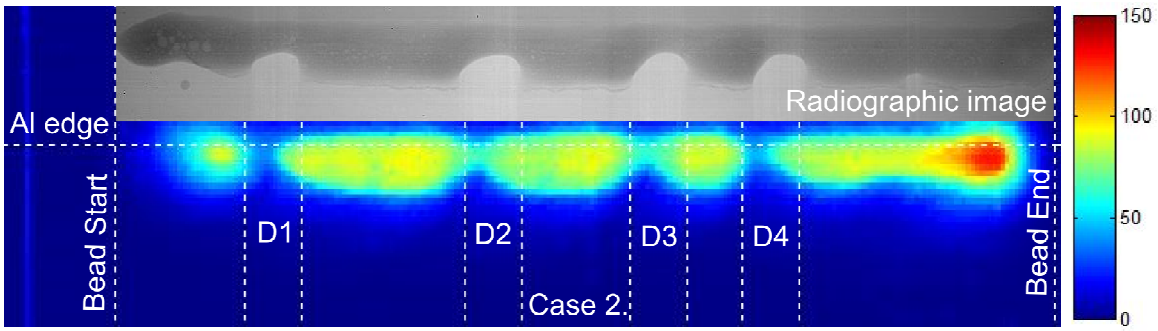

Figure 11. Reconstructed image of Case 1b compared with radiographic image

3. Conclusion

Real time monitoring of CMT welding brazing process using thermography technique by transmission mode of inspection has successfully demonstrated in this paper. Experiments were designed to identify the dependency of weld formation towards the presence of Zn coating on the steel plate and how effectively thermography can identify this effect. Two cases were considered for this purpose. The first case reveals the sensitivity of the IR thermography technique to identify a particular defect size. And it is observed that a no-zinc region of about 2 mm can be easily identified using the transmission mode of

measurement. The second case reveals the ability of thermography to resolve close-lying no-weld regions which is at a spacing of 5mm.

Acknowledgements

Authors express their sincere thanks to Mr. E Anbu Rasu, Technical Officer, International Advanced Research Centre for Powder Metallurgy and New Materials (ARCI), Hyderabad for his valuable assistance during the experiments and Mr. Raguvarun Kannaiyan, Project Officer, Indian Institute of Technology Madras for conducting the radiographic inspections on the weld samples.

References

[1] A. I. Taub, P. E. Krajewski, A. A. Luo, and J. N. Owens, "The evolution of technology for materials processing over the last 50 years: The automotive example," *JOM*, vol. 59, no. 2, pp. 48–57, Feb. 2007.

[2] W. . Miller, L. Zhuang, J. Bottema, a. . Wittebrood, P. De Smet, a Haszler, and a Vieregge, "Recent development in aluminium alloys for the automotive industry," *Mater. Sci. Eng. A*, vol. 280, no. 1, pp. 37–49, 2000.

[3] R. Borrisutthekul, T. Yachi, Y. Miyashita, and Y. Mutoh, "Suppression of intermetallic reaction layer formation by controlling heat flow in dissimilar joining of steel and aluminum alloy," *Mater. Sci. Eng. A*, vol. 467, no. 1–2, pp. 108–113, 2007.

[4] U. Dilthey and L. Stein, "Multimaterial car body design: challenge for welding and joining," *Sci. Technol. Weld. Join.*, vol. 11, no. 2, pp. 135–142, Mar. 2006.

[5] C. G. Pickin and K. Young, "Evaluation of cold metal transfer (CMT) process for welding aluminium alloy," vol. 11, no. 5, pp. 583–585, 2006.

[6] K. Furukawa, "New CMT arc welding process – welding of steel to aluminium dissimilar metals and welding of super-thin aluminium sheets," *Weld. Int.*, vol. 20, no. 6, pp. 440–445, 2006.

[7] R. Kozakov, H. Schöpp, G. Gött, A. Sperl, G. Wilhelm, and D. Uhrlandt, "Weld pool temperatures of steel S235 while applying a controlled short-circuit gas metal arc welding process and various shielding gases," *J. Phys. D. Appl. Phys.*, vol. 46, no. 47, p. 475501, 2013.

[8] P. W. Ramsey, J. J. Chyle, J. N. Kuhr, P. S. Myers, M. Weiss, and W. Groth, "Infrared temperature sensing systems for automatic fusion welding," *Weld. J.*, vol. 42, no. 8, pp. 337–346, 1963.

[9] C. J. Smith, "Self-adaptive control of penetration in a tungsten inert gas weld," *Adv. Weld. Process.*, pp. 272–282, 1974.

[10] N. H. Chin, B A Madsen and J. S. Goodlinc, "Infrared thermography for sensing the arc welding process," in *64th Annual AWS Convention, Philadelphia, Pennsylvania*, 1983, p. 227s–234s.

[11] D. Farson, R. Richardson, and X. Li, "Infrared Measurement of Base Temperature in Gas Tungsten Arc," *Weld. J.*, 1998.

[12] S.-H. Baik, M.-S. Kim, S.-K. Park, C.-M. Chung, C.-J. Kim, and K.-J. Kim, "Process monitoring of laser welding using chromatic filtering of thermal radiation," *Meas. Sci. Technol.*, vol. 11, no. 12, p. 1772, 2000.

[13] P. Huang, G. Zhang, Z. Wu, J. Cai, and Z. Zhou, "Inspection of defects in conductive multi-layered structures by an eddy current scanning technique: Simulation and experiments," *NDT E Int.*, vol. 39, no. 7, pp. 578–584, Oct. 2006.

[14] H. C. Wikle, S. Kottilingam, R. H. Zee, and B. A. Chin, "Infrared sensing techniques for penetration depth control of the submerged arc welding process," *J. Mater. Process. Technol.*, vol. 113, no. 1, pp. 228–233, 2001.

[15] B. Venkatraman, B. Venkatraman, M. Menaka, M. Menaka, M. Vasudevan, M. Vasudevan, B. Raj, and B. Raj, "Thermography for Online Detection of Incomplete Penetration and Penetration Depth Estimation," *Asia Pacific Conf. NDT*, 2006.

[16] Y. Zhang, *Real-time weld process monitoring*. Elsevier, 2008.

[17] U. Sreedhar, C. V. Krishnamurthy, K. Balasubramaniam, V. D. Raghupathy, and S. Ravisankar, "Automatic defect identification using thermal image analysis for online weld quality monitoring," *J. Mater. Process. Technol.*, vol. 212, no. 7, pp. 1557–1566, 2012.

[18] S. Yang, J. Zhang, J. Lian, and Y. Lei, "Welding of aluminum alloy to zinc coated steel by cold metal transfer," *Mater. Des.*, vol. 49, no. June, pp. 602–612, 2013.